Iraqi Journal of Scientific and Industrial Research
Volume 4, Issue 2, April-June 2025, pp. 55-62

Effects of Extraction Parameters on Particle Size of Silicon-Based Nanopowders Prepared by Physical Vapor Deposition Technique

Oday A. Hammadi [1], Athir A.R. Mahmud [2], Mohammed Y. Al-Azzawi [3]

[1] *Department of Physics, College of Education, Al-Iraqia University, Baghdad, IRAQ*
[2] *Department of Clinical Chemistry, College of Medicine, Al-Iraqia University, Baghdad, IRAQ*
[3] *Department of Biology, College of Education, Al-Iraqia University, Baghdad, IRAQ*

Abstract
In this work, the effects of different extraction parameters on the particle size of the nanopowders extracted from thin film samples of different silicon-based compounds were studied. These nanopowders were obtained by the conjunctional freezing-assisted ultrasonic extraction method. Thin films were different in their structures and their structural characteristics were determined. Results showed that extraction parameters such as freezing temperature, ultrasonic frequency and application time are very effective in determining the nanoparticle size, which is very important for many applications and uses of highly-pure nanomaterials and nanostructures.

Keywords: Nanopowders; Nanoparticles; Physical vapor deposition; Silicon compounds

Received: 2 January 2025; **Revised:** 17 February 2025; **Accepted:** 24 February 2025; **Published:** 1 April 2025

1. Introduction

Silicon compounds play a vital role in modern technology and industry due to their unique properties, such as thermal stability, electrical insulation, and chemical resistance [1-3]. Silica (SiO_2) is widely used in glass manufacturing, ceramics, and as a filler in rubber and plastics [4-6]. Silicones, a class of synthetic polymers, are essential in lubricants, sealants, medical implants, and waterproof coatings due to their flexibility and biocompatibility [7-10]. In electronics, silicon-based semiconductors (e.g., silicon carbide, SiC) are crucial for microchips, solar cells, and high-power devices due to their superior efficiency and thermal conductivity [11,12]. Silicon nitride (Si_3N_4) is used in cutting tools and aerospace components for its hardness and heat resistance [13,14].

Future developments focus on enhancing silicon-based materials for sustainable technologies [15-18]. Research is advancing silicon anodes for high-capacity lithium-ion batteries, improving energy storage for electric vehicles [19,20]. Silicon photonics is another emerging field, enabling faster data transmission in optical computing and telecommunications [21-25]. Additionally, nanotechnology is exploring silicon nanoparticles for drug delivery and environmental remediation [26,27].

In this work, the effects of some operation parameters of conjunctional freezing-assisted ultrasonic extraction method, such as freezing temperature, ultrasonic frequency and application time, on the particle size of extracted nanopowders are studied.

2. Experimental Part

A homemade dc reactive sputtering system employing a closed-field unbalanced dual magnetrons (CFUBDM) assembly was used to deposit nanostructured thin films on nonmetallic substrates. This system was used to prepare thin films from several compound materials, such as nickel oxide (NiO), silicon nitride (Si_3N_4), silicon dioxide (SiO_2), titanium dioxide (TiO_2), etc. [28-32]. The operation parameters and preparation conditions of these samples were separately optimized. More details on the specifications and operation of this system can be found elsewhere [33-38].

Highly-pure (99.99%) titanium sheet was used as a sputter target to be maintained on the cathode of the discharge system. Argon gas is used to generate discharge plasma while the oxygen, nitrogen or methane are used as reactive gases to form silicon compounds. The mixing ratio of argon and reactive gas could be precisely controlled in a gas mixer

© All Rights Reserved

before pumped into the deposition chamber. The discharge electrodes could be cooled using a cooling system employing water as a coolant. The crystalline phase of titanium dioxide nanostructures could be determined by controlling the operation parameters of magnetron sputtering system, especially gas mixing ratio, reactive gas content in the gas mixture, and anode temperature. Silicon dioxide nanostructures were prepared using Ar:O_2 gas mixture of 50:50. Silicon nitride nanostructures were prepared using Ar:N_2 gas mixture of 30:70. Silicon carbide nanostructures were prepared using Ar:CH_4 gas mixture of 70:30. Without cooling, the anode temperature might reach 150-180 °C. Using electrical heater on the anode can raise its temperature to 400 °C, which sufficiently induces the phase transformation. Therefore, the anode was cooled down to approximately 10 °C to avoid such transformation.

As the deposition time is varied, the thickness of the prepared film is proportionally varied. Film thickness was measured by laser-fringes method. The nanopowder was extracted from thin film samples by the conjunctional freezing-assisted ultrasonic extraction method. Full description and specifications of this method can be introduced in reference [39-41] and schematically shown in Fig. (1). The structural properties of the extracted nanopowders were determined by x-ray diffraction (XRD), scanning electron microscopy (SEM), and atomic force microscopy (AFM).

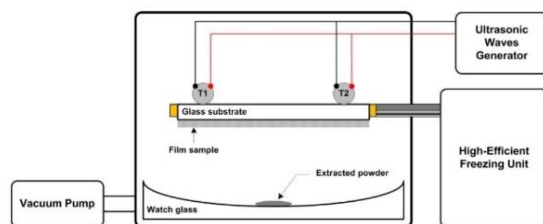

Fig. (1) Schematic diagram of the experimental setup of the conjunctional freezing-assisted ultrasonic extraction method used in this work [8]

3. Results and Discussion

Figure (2) shows the XRD patterns of the four different samples. As shown in Fig. (2a), a single-crystalline structure of silicon is recognized at 2θ = 28.25° corresponding to the crystal plane of (111) of silicon. Figure (2b) shows the XRD pattern of silicon carbide sample where three distinct diffraction peaks are observed at 2θ values of 32.58°, 42.64°, and 58.28°, those correspond to crystal planes of (111), (200), and (220), respectively, while the two peaks seen at 2θ of 22.84° and 46.80° correspond to the crystal planes of (010) and (210) of the H-rich SiC compound.

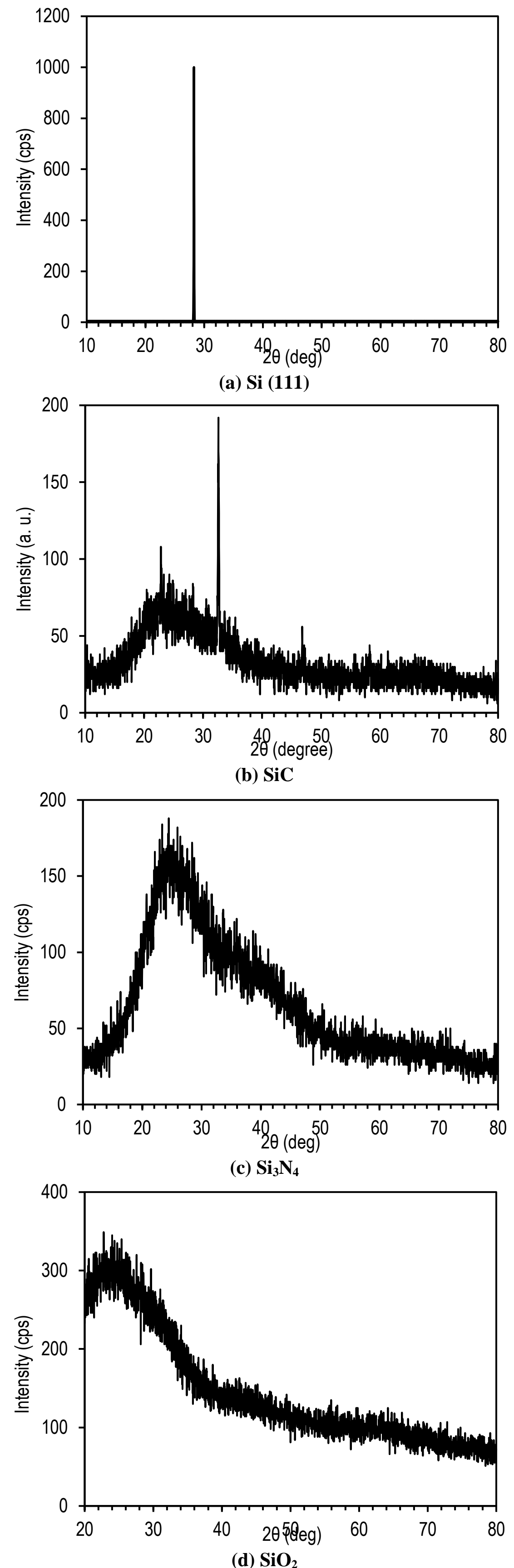

Fig. (2) XRD patterns of as-prepared Si-based samples (a) single-crystalline (111) Si, (b) SiC, (c) Si_3N_4, and (d) SiO_2

© All Rights Reserved

The existence of hydrogen cannot be completely avoided due to its strong trace in the reactive gas (CH_4). Figure (2c) indicate the XRd pattern of the silicon nitride (Si_3N_4) nanostructure, which shows amorphous structure. This structure is obvious for nanostructures due to the quantum size effect. A broad peak can be recognized at 2θ of 24.47°, which is corresponding to the crystal plane of (110) of α-phase of Si_3N_4. Figure (2d) shows the XRD pattern of silicon dioxide (SiO_2) sample, which exhibits an amorphous structure identifying the obvious silica structure in which a diffraction peak at 2θ of 24.0° is distinguished.

Figure (3) shows the FE-SEM images of the four different silicon compounds prepared in this work. Figure (3a) shows the morphology of the as-prepared silicon sample. Approximately spherical particles can be seen with uniform distribution and no aggregation over the surface. These characteristics are obvious for the nanostructures prepared from single-crystalline silicon target using sputtering technique [42-45]. In Fig. (3b), the surface morphology of the silicon carbide (SiC) sample shows reasonable differences in the aggregated particles with minimum particle size of about 19 nm. It is clear that the distribution of particles is not uniform and apparent voids are observed. Figure (3c) shows the surface morphology of the silicon nitride (Si_3N_4) sample as spherical particles are apparently seen with a wide range of sizes. As well, no aggregation is seen that is an obvious nature of ceramic materials. Figure (3d) shows the surface morphology of silicon dioxide (SiO_2) sample where a minimum particle size of 34.55 nm can be seen with completely aggregated particles forming clusters over the surface. The morphology of this sample is very similar to that of the as-prepared silicon when compared to the other two compounds (SiC and Si_3N_4).

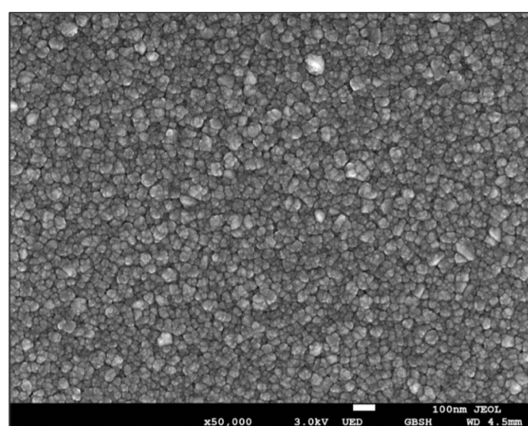

(a) (111) Si

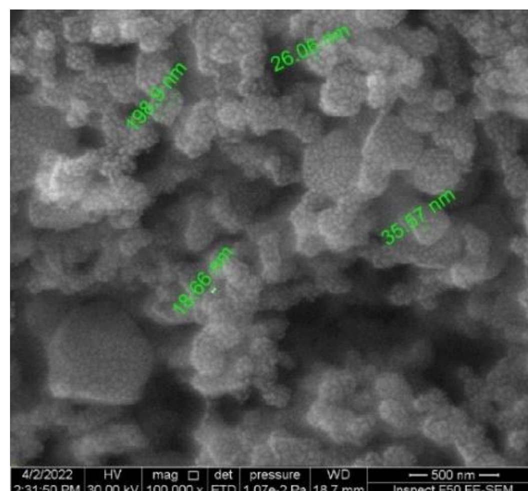

(b) SiC

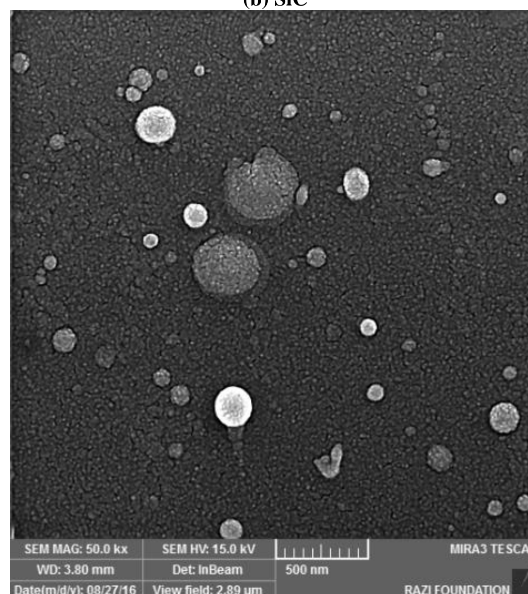

(c) Si_3N_4

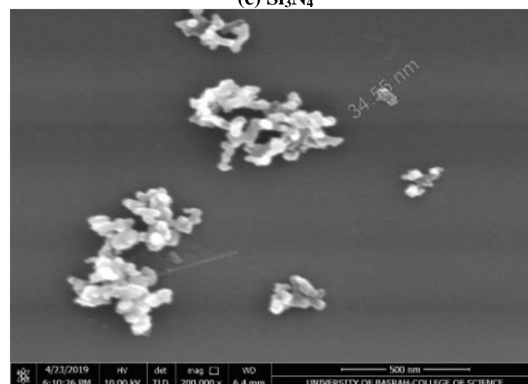

(d) SiO_2

Fig. (3) FE-SEM images of as-prepared Si-based samples (a) single-crystalline (111) Si, (b) SiC, (c) Si_3N_4, and (d) SiO_2

Figure (4) shows the atomic force microscope (AFM) images of (111) Si, SiC, Si_3N_4, and SiO_2 nanostructures prepared in this work. These images reveals distinct surface morphologies and roughness characteristics for these samples. The (111) Si sample exhibits a smooth surface with atomic steps due to its crystalline nature with low roughness, however,

© All Rights Reserved

Iraqi Journal of Scientific and Industrial Research
Volume 4, Issue 2, April-June 2025, pp. 55-62

defects or contamination may increase roughness. The silicon carbide (SiC) samples shows higher surface roughness due to its hard, polycrystalline structure. The grain boundaries and sputtering-induced defects contribute to irregular topography. The silicon nitride (Si_3N_4) sample with amorphous or nanocrystalline, shows moderate roughness and uniform grain distribution but may have pinholes or voids from deposition stresses. The silicon dioxide (SiO_2) sample shows typically smooth due to its glassy, amorphous nature and may show slight granularity from sputtering conditions. The key differences between these samples are discussed by the crystalline versus amorphous structures, as (111) Si is atomically flat, while Si_3N_4 and SiO_2 are smoother but lack long-range order. Also, hardness has a reasonable effect as the high hardness of SiC leads to pronounced grain contrast [46-48]. Finally, the deposition effects may impose differences as sputtering parameters (power, pressure) influence grain size and defects in SiC and Si_3N_4 more than in SiO_2.

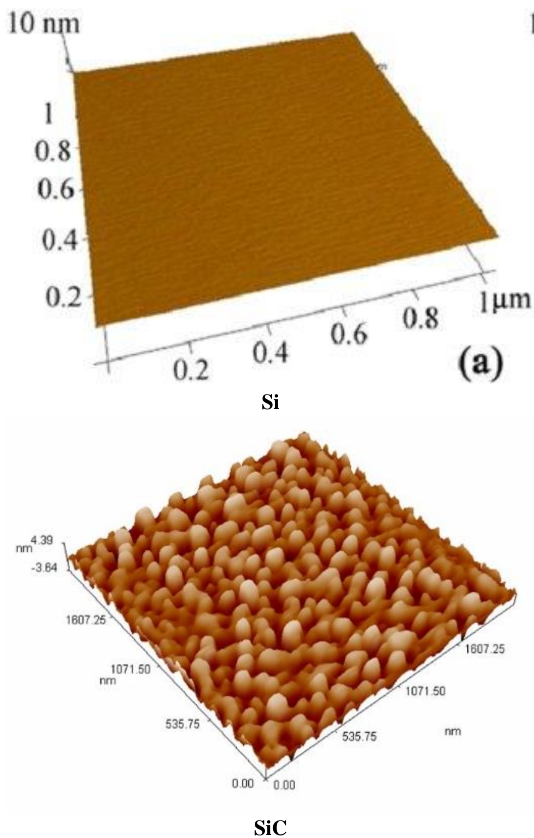

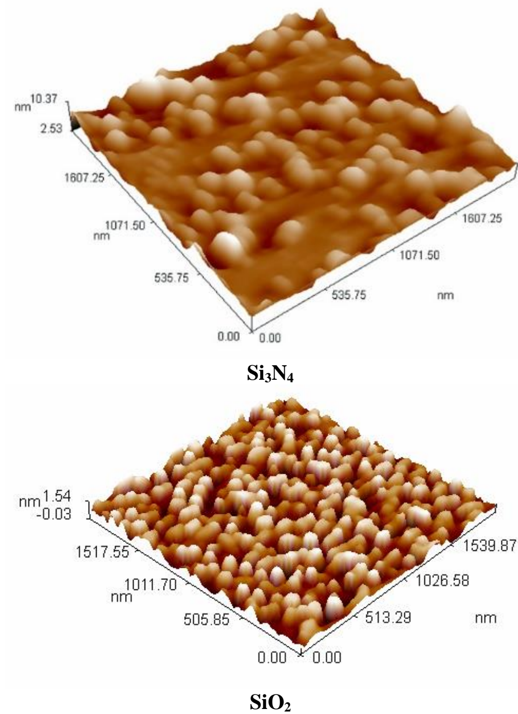

Fig. (4) AFM images of as-prepared Si-based samples (a) single-crystalline (111) Si, (b) SiC, (c) Si_3N_4, and (d) SiO_2

Figure (5) shows the variation of nanoparticle size of the four different samples prepared in this work with the deposition time, which determines film thickness. As the deposition time is increased, the film thickness is increased and hence the layers of the thin film are further grown. This growth results in the grains to get larger as observed in this figure. Silicon dioxide and silicon carbide structures exhibit higher increase in nanoparticle size than those of silicon and silicon nitride structures, which in turn show highly stability in particle size. This is attributed to the thermally-induced growth of grains in the deposited films [49-51].

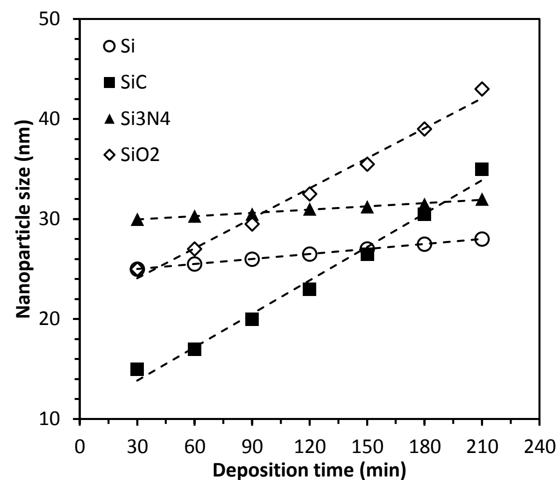

Fig. (5) Variation of nanoparticle size with deposition time for the four different silicon-based nanostructures prepared in this work

© All Rights Reserved

As the nanopowders were extracted from the thin film samples using the conjunctional freezing-assisted ultrasonic extraction method, the effect of freezing temperature on the value of ultrasonic frequency at which the nanopowder was completely extracted is shown in Fig. (6). As the freezing temperature is decreased, lower frequency is required to extract the nanopowder because lower freezing temperature lead to further shrinkage of the nonmetallic substrate and hence the adhesion of the film to the substrate gets lower.

It is clear that the values of ultrasonic frequencies required for the extraction of nanopowders are relatively convergent regardless the grown phase of silicon compound, however, the silicon nitride samples needed for higher frequencies due to the thermal effect leading to better adhesion between the film and the substrate [52-55].

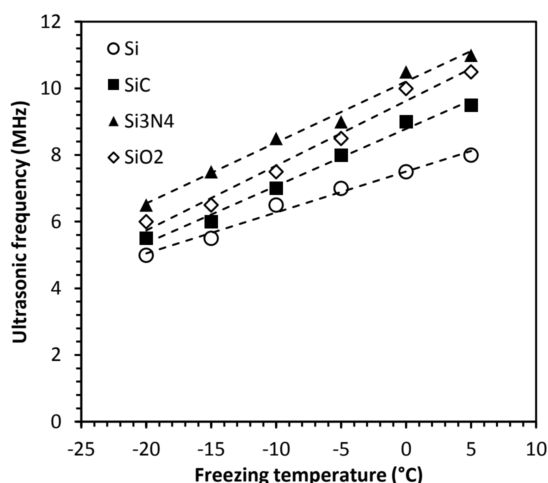

Fig. (6) Variation of ultrasonic frequency with freezing temperature for the four different silicon-based nanostructures prepared in this work

The variation of nanoparticle size with the ultrasonic frequency at which the nanopowder was extracted for the four types of silicon-based structures prepared in this work is shown in Fig. (7). As the thin film is typically composed of at least several layers of silicon compound particles, higher ultrasonic frequency can vibrate atoms in different layers and hence extract larger particles. As the silicon nitride contains larger grains than other three materials due to thermal effect, their extracted particles are larger than those of the silicon dioxide and silicon carbide samples at the same value of ultrasonic frequency.

The time taken to apply the ultrasonic waves to the thin films sample before the extraction of nanopowder was completed is an effective parameter. Accordingly, the variation of nanoparticle size with application time at frequency of 5 MHz is shown in Fig. (8) for the four silicon-based thin films. It is clearly observed that the particle size of the extracted nanopowder does not show large differences for application times from 30 to 210 minutes. This is attributed to the fact that particles of certain size are extracted by ultrasonic waves of given frequency regardless of the application time [56]. Extraction of particles containing molecules from different layers within the thin film is carried out at certain range of sizes as a function of ultrasonic frequency. In case of silicon nitride structure, larger particles are extracted due to their further growth within the deposited film.

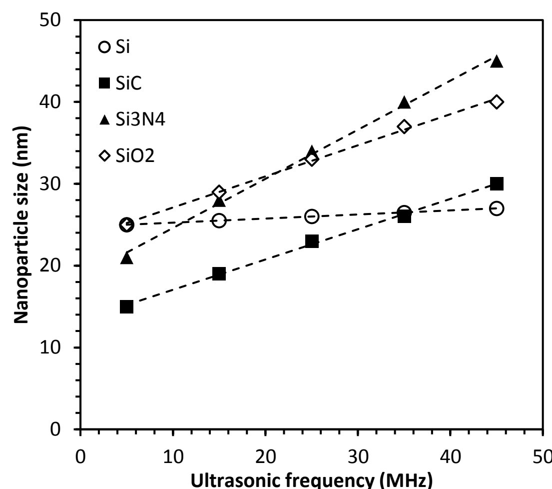

Fig. (7) Variation of nanoparticle size with the ultrasonic frequency for the four different silicon-based nanostructures prepared in this work

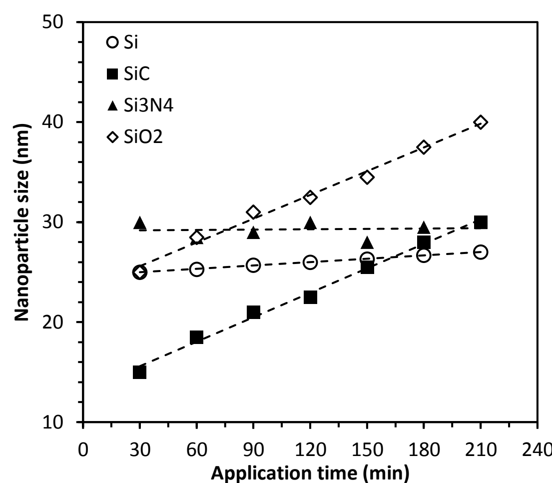

Fig. (8) Variation of nanoparticle size with the application time of ultrasonic waves for the four different silicon-based nanostructures prepared in this work

As the extraction method mainly depends on the freezing stage, the freezing temperature may be very effective in determining the particle size of the extracted nanopowder. Figure (9) shows the variation of nanoparticle size with freezing temperature for the four types of silicon-based samples prepared in this work. It was mentioned before that the lower freezing temperature leads to larger shrinkage in the substrate on which the thin film is deposited and hence the adhesion between the film and the substrate gets lower and the film surface breaks earlier at the same

© All Rights Reserved

value of ultrasonic frequency. Accordingly, larger particles can be extracted from the thin film before partitioning into smaller ones. In contrast, freezing to relatively higher temperatures leads to smaller shrinkage in the substrate and the adhesion between the film and the substrate gets higher. Therefore, the application of ultrasonic waves can extract particles from the upper surface layer of the thin film, which means smaller particles [57,58]. Layer-by-layer extraction at higher freezing temperatures produces smaller nanoparticles when compared to the case of lower temperatures.

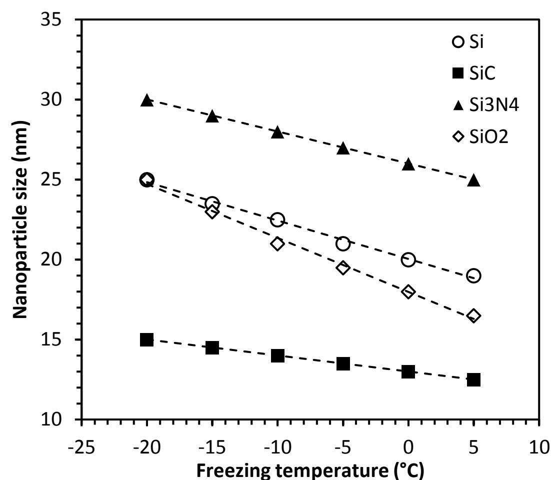

Fig. (9) Variation of nanoparticle size with the freezing temperature for the four different silicon-based nanostructures prepared in this work

4. Conclusion

As conclusions, freezing temperature, ultrasonic frequency and the time taken to apply ultrasonic waves on nanostructured thin films deposited on nonmetallic substrates are very effective to determine the nanoparticle size of nanopowders extracted from these thin film samples. The conjunctional freezing-assisted ultrasonic extraction method can be successfully used to extract highly-pure nanoparticles with approximately the same size of nanoparticles in the thin films deposited by physical vapor deposition methods and techniques. This technique is reliable, efficient and low cost to produce highly-pure nanomaterials with as low as possible particle sizes.

References

[1] C. Yanyan and J. Gang ,"Refractive Index and Thickness Analysis of Natural Silicon Dioxide Film Growing on Silicon with Variable-Angle Spectroscopic Ellipsometry", Spectroscopy, 26(21) (2006) 10.

[2] A. Ranjgar, R. Norouzi, A. Zolanvari and H. Sadeghi, “Characterization and Optical Absorption Properties of Plasmonic Nanostructured Thin Films”, Armenian J. Phys., 6(4) (2013) 198-203.

[3] O.A. Hamadi, “Characteristics of CdO-Si heterostructure produced by plasma-induced bonding technique,” Proc. IMechE Part L: J. Mater. Design and Applications, 222, 2008, 65–71.

[4] A. Tabata, N. Matsuno, Y. Suzuoki, T. Mizutani, “Optical properties and structure of SiO_2 films prepared by ion-beam sputtering”, Thin Solid Films, 289 (1996) 84-89.

[5] A.A. Issa, “The Effect of Annealing on Nano-Topography of SiO_2 Film”, Raf. J. Sci., 25(2) (2014) 74-86.

[6] A.K. Saadon, “The Effect of Silica SiO_2 on the Dielectric and Physical Properties of Mn-Ni Ferrite”, Ibn Al-Haitham J. for Pure and Appl. Sci., 25(3) (2012) 186-191.

[7] A.K. Yousif and O.A. Hamadi, “Plasma-induced etching of silicon surfaces,” Bulg. J. Phys., 35(3), 2008, 191–197.

[8] A.M. Al-Dhafiri, “High-Quality Plasma-Induced Crystallization of Amorphous Silicon Structures”, Iraqi J. Appl. Phys., 5(1), 2009, 35-39.

[9] A.T.S. Yee, “Synthesis of Silicon Nanowires by Selective Etching Process”, Iraqi J. Appl. Phys., 4(3), 2008, 15-17.

[10] Adivarahan V, Simin G, Yang JW, Lunev A, Khan MA, Pala N, Shur M, Gaska R, “SiO_2 passivated lateral-geometry GaN transparent Schottky-barrier detectors”, Appl. Phys. Lett., 77 (2000) 863-865.

[11] Alexandrov SE, McSporran N, Hitchman ML, “Remote AP-PECVD of silicon dioxide films from hexamethyldisiloxane (HMDSO)”, Chem. Vap. Depos., 11 (2005) 481-490.

[12] Bang SB, Chung TH, Kim Y, Kang MS, Kim JK, “Effects of the oxygen fraction and substrate bias power on the electrical and optical properties of silicon oxide films by plasma enhanced chemical vapour deposition using $TMOS/O_2$ gas”, J. Phys. D: Appl. Phys., 37 (2004) 1679-1684.

[13] Choi J-K, Kim D, Lee J, Yoo J-B, “Effects of process parameters on the growth of thick SiO_2 using plasma enhanced chemical vapor deposition with hexamethyldisilazane”, Surf. Coat. Technol., 131 (2000) 136-140.

[14] Croci S, Pecheur A, Autran JL, Vedda A, Caccavale F, Martini M, Spinolo G, “SiO_2 films deposited on silicon at low temperature by plasma-enhanced decomposition of hexamethyldisilazane: defect characterization”, J. Vac. Sci. Technol. A Vac. Surf. Film, 19 (2001) 2670-2675.

[15] E.S.M. Goh, T.P. Chen, C.Q. Sun and Y.C. Liu, “Thickness effect on the band gap and optical properties of germanium thin films”, J. Appl. Phys., 107 (2010) 024305. DOI: 0021-8979/2010/107(2)/024305/5/$30.00

[16] H. Jung, W.H. Kim, I.K. Oh, C.W. Lee, C.

© All Rights Reserved

Lansalot-Matras, S.J. Lee, J.M. Myoung, H.B. Ram Lee and H. Kim, "Growth characteristics and electrical properties of SiO2 thin films prepared using plasma-enhanced atomic layer deposition and chemical vapor deposition with an aminosilane precursor", J. Mater. Sci., 51(11) (2016) 5082-5091. DOI 10.1007/s10853-016-9811-0

[17] D. Hiller, R. Zierold, J. Bachmann, M. Alexe, Y. Yang, J.W. Gerlach, A. Stesmans, M. Jivanescu, U. Müller, J. Vogt, H. Hilmer, P. Löper, M. Künle, F. Munnik, K. Nielsch, and M. Zacharias, "Low temperature silicon dioxide by thermal atomic layer deposition: investigation of material properties", J. Appl. Phys., 107 (2010) 064314-1–064314-10.

[18] Y. Inoue and O. Takai, "Spectroscopic studies on preparation of silicon oxide films by PECVD using organosilicon compounds", Plasma Sources Sci. Technol., 5 (1996) 339-343.

[19] J.P. Bange, L.S. Patil and D.K. Gautam, "Growth and characterization of SiO_2 films deposited by flame hydrolysis deposition system for photonic device application", Prog. in Electromag. Res. M, 3 (2008) 165–175.

[20] S. Kamiyama, T. Miura and Y. Nara, "Comparison between SiO_2 films deposited by atomic layer deposition with $SiH_2[N(CH_3)_2]_2$ and $SiH[N(CH_3)_2]_3$ precursors", Thin Solid Films, 515 (2006) 1517-1521.

[21] J.W. Klaus and S.M. George, "Atomic layer deposition of SiO_2 at room temperature using NH3-catalyzed sequential surface reactions", Surf. Sci., 447 (2000) 81-90.

[22] J.W. Klaus, A.W. Ott, J.M. Johnson, and S.M. George, "Atomic layer controlled growth of SiO_2 films using binary reaction sequence chemistry", Appl. Phys. Lett., 70 (1997) 1092–1094.

[23] J.W. Klaus, O. Sneh, A.W. Ott, and S.M. George, "Atomic layer deposition of SiO_2 using catalyzed and uncatalyzed selflimiting surface reactions", Surf. Rev. Lett., 06 (1999) 435-448.

[24] M. Yu, H. Qiu, X. Chen, P. Wu and Y. Tian, "Comparative study of the characteristics of Ni films deposited on SiO_2/Si(100) by oblique-angle sputtering and conventional sputtering", 516 (2008) 7903-7909.

[25] M.A. Hameed and Z.M. Jabbar, "Preparation and Characterization of Silicon Dioxide Nanostructures by DC Reactive Closed-Field Unbalanced Magnetron Sputtering", Iraqi J. Appl. Phys., 12(4), 2016, 13-18

[26] P. Pan, "The composition and properties of PECVD silicon oxide films", J. Electrochem. Soc., 132 (1985) 2012–2019.

[27] S.M. Zayed, A.M. Alshimy and A.E. Fahmy, "Effect of Surface Treated Silicon Dioxide Nanoparticles on Some Mechanical Properties of Maxillofacial Silicone Elastomer", Int. J. Biomater., 2014, article 750398, http://dx.doi.org/10.1155/2014/750398

[28] I. Suzuki, C. Dussarrat, and K. Yanagita, "Extra low-temperature SiO_2 deposition using aminosilanes", ECS Trans., 3 (2007) 119-128.

[29] T. Tamura, S. Ishibashi, S. Tanaka, M. Kohyama and M.H. Lee, "First-principles analysis of optical absorption edge in pure and fluorine-doped SiO_2 glass", Comput. Mater. Sci., 44 (2008) 61-66.

[30] W.F. Wu and B.S. Chiou, "Optical and mechanical properties of reactively sputtered silicon dioxide films", Semicond. Sci. Technol. 11 (1996) 1317-1321.

[31] K.Z. Yahiya et al., "Properties of Silicon Carbide Thin Films Deposited by Vacuum Thermal Evaporation", J. of Semicond. Technol. Sci., 5(3) (2005) 182-186.

[32] O.A. Hamadi and K.Z. Yahiya, "Optical and electrical properties of selenium-antimony heterojunction formed on silicon substrate", Sharjah Univ. J. Pure Appl. Sci., 4(2) (2007) 1-11.

[33] S.M. Hussain et al., "Normalized Characteristics of Laser-Induced Diffusion of Arsenic Dopants in Silicon", Eng. Technol. J., 25(4) (2007) 584-590.

[34] A.K. Yousif et al., "Plasma-Induced Etching of Silicon Surfaces", Bulg. J. Phys., 35(3) (2008) 191-197.

[35] B.A.M. Bader et al., "Electrical Characteristics of Silicon p-n Junction Solar Cells Produced by Plasma-Assisted Matrix Etching Technique", Eng. Technol. J., 26(8) (2008) 995-1001.

[36] O.A. Hamadi, "Profiling of Antimony Diffusivity in Silicon Substrates using Laser-Induced Diffusion Technique", Iraqi J. Appl. Phys. Lett., 3(1) (2010) 23-26.

[37] O.A. Hammadi, "Photovoltaic Properties of Thermally-Grown Selenium-Doped Silicon Photodiodes for Infrared Detection Applications", Phot. Sen., 5(2) (2015) 152-158.

[38] M.K. Khalaf et al., "Fabrication of UV Photodetector from Nickel Oxide Nanoparticles Deposited on Silicon Substrate by Closed-Field Unbalanced Dual Magnetron Sputtering Techniques", Opt. Quantum Electron., 47(12) (2015) 3805-3813.

[39] M.K. Khalaf et al., "Fabrication and Characterization of UV Photodetectors Based on Silicon Nitride Nanostructures Prepared by Magnetron Sputtering", Proc. IMechE, Part N, J. Nanomater. Nanoeng. Nanosys., 230(1) (2016) 32-36.

[40] O.A. Hammadi, "Characteristics of Heat-Annealed Silicon Homojunction Infrared Photodetector Fabricated by Plasma-Assisted Technique", Phot. Sen., 6(4) (2016) 345-350.

© All Rights Reserved ISSN (print) 2079-4630 (online) 3079-2371

[41] O.A. Hamadi, "Characterization of SiC/Si Heterojunction Fabricated by Plasma-Induced Growth of Nanostructured Silicon Carbide Layer on Silicon Surface", Iraqi J. Appl. Phys., 12(2) (2016) 9-13.
[42] F.J. Kadhim and A.A. Anber, "Highly-Pure Nanostructured Silicon Nitride Films Prepared by Reactive DC Magnetron Sputtering", J. Indust. Eng. Sci., 25(5) (2016) 91-94.
[43] M.A. Hameed and Z.M. Jabbar, "Preparation and Characterization of Silicon Dioxide Nanostructures by DC Reactive Closed-Field Unbalanced Magnetron Sputtering", Iraqi J. Appl. Phys., 12(4) (2016) 13-18.
[44] M.K. Khalaf et al., "Silicon Nitride Nanostructures Prepared by Reactive Sputtering Using Closed-Field Unbalanced Dual Magnetrons", Proc. IMechE, Part L, J. Mater.: Design & Appl., 231(5) (2017) 479-487.
[45] F.J. Kadhim and A.A. Anber, "Fabrication of Nanostructured Silicon Nitride Thin Film Gas Sensors by Reactive DC Magnetron Sputtering", Proc. IMechE, Part N, J. Nanomater. Nanoeng. Nanosys., 231(4) (2017) 173-178.
[46] A.A. Anber and F.J. Kadhim, "Preparation of Nanostructured Si_xN_{1-x} Thin Films by DC Reactive Magnetron Sputtering for Tribology Applications", Silicon, 10 (2018) 821-824.
[47] M.A. Hameed and Z.M. Jabbar, "Optimization of Preparation Conditions to Control Structural Characteristics of Silicon Dioxide Nanostructures Prepared by Magnetron Plasma Sputtering", Silicon, 10(4) (2018) 1411-1418.
[48] B.K. Nasser and M.A. Hameed, "Narrow Emission Linewidth of Highly-Pure Silicon Nitride Nanoparticles in Different Dye Solutions as Random Gain Media", Nonl. Opt. Quantum. Opt., 53(1-2) (2019) 99-105.
[49] D.A. Taher and M.A. Hameed, "Spectroscopic Characteristics of Silicon Nitride Thin Films Prepared by DC Reactive Sputtering Using Silicon targets with Different Types of Conductivity", *Iraqi J. Appl. Phys.*, 19(4A) (2023) 73-76.
[50] B.K. Nasser and M.A. Hameed, "Structural Characteristics of Silicon Nitride Nanostructures Synthesized by DC Reactive Magnetron Sputtering", Iraqi J. Appl. Phys., 15(4) (2019) 33-36.
[51] H.G. Fahad et al., "Characterization of Highly-Pure Silicon Dioxide Nanoparticles as Scattering Centers for Random Gain Media", Iraqi J. Appl. Phys., 16(2) (2020) 37-42.
[52] N.H. Mutesher and F.J. Kadhim, "Comparative Study of Structural and Optical Properties of Silicon Dioxide Nanoparticles Prepared by DC Reactive Sputtering and Sol-Gel Route", Iraqi J. Appl. Phys., 17(1) (2021) 17-20.
[53] F.J. Kadhim et al., "Spectroscopic Study of Chromium-Doped Silicon Nitride Nanostructures Prepared by DC Reactive Magnetron Sputtering", Iraqi J. Appl. Phys., 17(2) (2021) 9-12.
[54] O.A. Hammadi, "New Technique to Synthesize Silicon Nitride Nanopowder by Discharge-Assisted Reaction of Silane and Ammonia", Mater. Res. Exp., 8(8) (2021) 085013.
[55] O.A. Hammadi, "Magnetically-Supported Electrically-Induced Formation of Silicon Carbide Nanostructures on Silicon Substrate for Optoelectronics Applications", Opt. Quantum Electron., 54(7) (2022) 427.
[56] D.A. Taher and M.A. Hameed, "Structural and Hardness Characteristics of Silicon Nitride Thin Films Deposited on Metallic Substrates by DC Reactive Sputtering Technique", *Silicon*, 15 (2023) 7855-7864.
[57] O.A. Hammadi, "Production of Nanopowders from Physical Vapor Deposited Films on Nonmetallic Substrates by Conjunctional Freezing-Assisted Ultrasonic Extraction Method", Proc. IMechE, Part N, J. Nanomater. Nanoeng. Nanosys., 232(4) (2018) 135-140.
[58] O.A. Hammadi, "Conjunctional Freezing-Assisted Ultrasonic Extraction of Silicon Dioxide Nanopowders from Thin Films Prepared by Physical Vapor Deposition Technique", Iraqi J. Appl. Phys., 15(4) (2019) 23-28.

© All Rights Reserved
ISSN (print) 2079-4630 (online) 3079-2371